第 33 卷第 7 期
2017 年 7 月

无 机 化 学 学 报
CHINESE JOURNAL OF INORGANIC CHEMISTRY

Vol.33 No.7
1305-1312

# 基于 2,5-噻吩二甲酸的钙(Ⅱ)和钡(Ⅱ)配位聚合物的合成、晶体结构及性质

张雁红*,[1] Adhikari Shiba Prasad[2] Day Cynthia[2] Lachgar Abdou*,[2]

([1]内蒙古师范大学化学与环境科学学院,内蒙古自治区绿色催化重点实验室,呼和浩特 010022)

([2]维克森林大学化学系,美国北卡罗莱纳州,NC 27109)

**摘要**:在溶剂热条件下,合成了 2 个碱土金属配位聚合物$[Ca(tdc)(DMF)_2]_n$ (**1**)和$[Ba(tdc)]_n$ (**2**)($H_2tdc$=2,5-噻吩二甲酸),分别用元素分析、红外光谱、X 射线单晶衍射、粉末衍射、热重分析和荧光光谱对它们进行了表征。结构分析表明,配合物 **1** 具有 4,4 连接的二维层状结构,拓扑符号为$(4^4\cdot6^2)$,而配合物 **2** 呈现三维网络结构。固体荧光测试表明配合物 **1** 比配合物 **2** 具有更显著的荧光性能。

**关键词**:配位聚合物;碱土金属;晶体结构;荧光

**中图分类号**:O614.23+1;O614.23+3 **文献标识码**:A **文章编号**:1001-4861(2017)07-1305-08

**DOI**:10.11862/CJIC.2017.158

## Syntheses, Crystal Structures and Characterization of Ca(Ⅱ) and Ba(Ⅱ) Coordination Polymers Derived from Thiophene-2,5-dicarboxylate

ZHANG Yan-Hong*,[1] Adhikari Shiba Prasad[2] Day Cynthia[2] Lachgar Abdou*,[2]

([1]*College of Chemistry and Environment Science, Inner Mongolia Key Laboratory of Green Catalysis, Inner Mongolia Normal University, Hohhot* 010022, *China*)

([2]*Department of Chemistry, Wake Forest University, Winston-Salem, NC* 27109, *USA*)

**Abstract:** Two new alkaline earth metal coordination polymers $[Ca(tdc)(DMF)_2]_n$ (**1**) and $[Ba(tdc)]_n$ (**2**) ($H_2tdc$=2,5-thiophene dicarboxylate) have been synthesized under solvothermal condition. They were characterized by elemental analysis, IR spectroscopy, single crystal X-ray diffraction, powder X-ray diffraction, thermogravimetric analysis, and fluorescent analysis. Complex **1** exhibits a two-dimensional (2D) layer structure with a uninodal (4,4)-connected $(4^4\cdot6^2)$ topological type; whereas, complex **2** features a 3D framework consisting of elongated hexagonal channels. Solid-state photoluminescent properties indicate that complex **1** shows noticeable fluorescent emissions upon excitation in comparison to that of complex **2**. CCDC: 1509673, **1**; 1509674, **2**.

**Keywords:** coordination polymer; alkaline earth metal; crystal structure; fluorescence

## 0 Introduction

The design and synthesis of metal-organic coordination polymers (MOCPs) have attracted considerable attention due to their appealing structural, topological novelty and potential applications in functional materials such as storage, separation, catalysis, luminescence, ion exchange, drug delivery, electrical conductivity, and molecular magnetism[1-13]. Although many efforts and great progress have been made in the construction of diverse architectures, the rational design and controllable preparation of the coordination

收稿日期:2017-03-08。收修改稿日期:2017-05-27。

内蒙古自治区自然科学基金(No.2014BS0206)和国家留学基金委(No.201408155050)资助项目。

*通信联系人。E-mail:zhangyh@imnu.edu.cn,lachgar@wfu.edu

polymers still remain a great challenge in the field of crystal engineering. It is well known that the assembly process of MOCPs is deeply influenced by many factors, such as connectivity of organic building blocks or metal ions, solvents, molar ratio of reactants, temperature, the counter anions, pH value and so on[14-17]. Of all these, the judicious selection of organic linkers, such as flexibility, shape, length, steric effects, and substituent group is crucial to the structural architectures and functionalities of MOCPs. Polycarboxylic ligands are considered to be good candidates because of their versatile coordination modes[18-22]. Although a substantial number of coordination polymers incorporating various kinds of aromatic polycarboxylic acids and even including N-heterocyclic derivatives have been reported, there have been far less focus on the investigation of S-containing polycarboxylic acid ligands. Out of the different carboxylate based ligands, 2,5-thiophene dicarboxylate ($H_2$tdc) has two carboxyl groups that may be completely or partially deprotonated, leading to abundant coordination modes and readily adjustable geometries to different metal centers[23-28]. The unique V-shaped arrangement of this ligand between the two carboxyl groups enables non-centrosymmetric structures, which is a prerequisite for preparing nonlinear optical materials. Furthermore, the lone electron pair of the hetero-S atom in the $H_2$tdc ligand is more likely delocalized within the thiophene ring and can easily promote charge transfer associated with the target coordination polymers[29]. It is expected to be an important intermediate in the development of photoluminescent materials.

On the other hand, in contrast to abundant research in *d*-block transition metal or *f*-block rare earth metal polymers, the coordination behavior and potential applications of alkaline earth metal coordination polymers have remained largely an unexplored area due to their relatively weak complexing ability[30]. However, alkaline earth metal ions have considerable advantage for constructing MOCPs, such as low molecular weight, high charge density plus the relative abundance with low cost. Out of the different alkaline earth metals, magnesium and calcium perform numerous biological functions in all life forms and some Mg and Ca-based MOFs exhibit exceptional gas adsorption properties and photoluminescence properties[31]. Barium and strontium metals have been known as antagonists for potassium and calcium, respectively[32].

Taking into account all these contexts, we have strategically combined 2,5-thiophenedicarboxylate ($H_2$tdc) organic linker with alkaline earth metal ions to build new metal-organic coordination polymers. In the present paper, two new polymers, namely, $[Ca(tdc)(DMF)_2]_n$ (**1**) and $[Ba(tdc)]_n$ (**2**) have been successfully synthesized. Their single crystal structures, solid state thermal studies and fluorescent properties have also been investigated.

## 1 Experimental

### 1.1 Materials and physical measurements

All reagents used in the syntheses were commercially available and used as purchased. Elemental analyses for C, H, N, S were performed on a LECO CHNS-932 Elemental Analyzer. FT-IR spectra were recorded using KBr pellet on a Perkin Elmer Spectrum 100 Spectrometer in the 4 000~600 $cm^{-1}$ region. The powder X-ray diffraction (PXRD) data were collected on a Bruker D2 PHASER equipped with a graphite monochromator using Cu $K\alpha$ radiation ($\lambda$ = 0.154 060 nm) in $2\theta$ range of 7°~50° at room temperature, operated at 30 kV and 10 mA. Thermogravimetric analyses (TGA) were performed on a SDT Q600 V20.9 Build 20 analyzer under nitrogen atmosphere with a heating rate of 10 ℃·$min^{-1}$ in the range of 30~800 ℃. The fluorescence spectra were measured on a FLS920 fluorescence spectrophotometer.

### 1.2 Synthesis of the complex $[Ca(tdc)(DMF)_2]_n$ (1)

A mixture of $CaCl_2·4H_2O$ (18.3 mg, 0.10 mmol) and $H_2$tdc (17.2 mg, 0.10 mmol) was dissolved in 5 mL of DMF/$H_2O$ (4∶1, *V*/*V*) in a 10 mL glass vial. After ultrasonication for about 30 min, the resulting solution was placed in an autoclave and heated at 90 ℃ for 5 days. After the mixture was slowly cooled to room temperature, a large amount of colorless block crystals of **1** were collected. (Yield: 69% based on

Ca). Elemental analysis Calcd. for $C_{12}H_{16}CaN_2O_6S$(%): C, 40.44; H, 4.52; N, 7.86; S, 8.99. Found (%): C, 40.39; H, 4.60; N, 7.80; S; 8.94. FT-IR (KBr pellet, $cm^{-1}$) selected bands: 1 597(s), 1 564(s), 1 524(m), 1 457(w), 1 355(s), 1 332(s), 1 251(w), 1217(w), 1 121 (m), 1 035(m), 847(w), 776(s), 683(m).

### 1.3 Synthesis of the complex [Ba(tdc)]$_n$ (2)

Complex **2** was synthesized with the same procedure as that of **1**, except that $CaCl_2\cdot4H_2O$ was substituted with $BaBr_2\cdot2H_2O$. Light yellow crystals of **2** were obtained after filtration, washed with DMF, and dried in air. The yield was 60% based on Ba. Elemental analysis Calcd. for $C_6H_2BaO_4S$(%): C, 23.44; H, 0.66; S, 10.43. Found(%): C, 23.54; H, 0.75; S, 10.38. FT-IR (KBr pellet, $cm^{-1}$) selected bands: 1 517(s), 1 457 (w), 1 360(s), 1 334(m), 1 316(m), 1 248(m), 1 215(w), 1 126(w), 1 043(m), 849(w), 805(s), 772(s), 683(m).

### 1.4 X-ray crystallographic studies

The single crystals of complexes **1** and **2** were mounted on a Bruker SMART APEX CCD with graphite-monochromatized Mo $K\alpha$ radiation ($\lambda$=0.071 073 nm) by using the $\omega$ scan technique at 193 K. Empirical absorption corrections were applied by using the SADABS program[33]. The structures were solved by direct methods and refined by the full-matrix least-squares on $F^2$ with anisotropic thermal parameters for all non-hydrogen atoms[34]. All hydrogen atoms were added in idealized positions and refined isotropically. Further details of the structure analysis were summarized in Table 1. Selected bond lengths and bond angles are listed in Table 2. In complex **2**, the sulfur atom of the thiophene ring shows serious disorder over two positions and was refined in two complementary positions with 0.94 and 0.06 occupancies. Regardless of the disorder problems, the results are clearly sufficient to establish the connectivity of the molecule without any ambiguity.

CCDC: 1509673, **1**; 1509674, **2**.

**Table 1　Crystal data and structure refinement for the complexes**

| Complex | 1 | 2 |
|---|---|---|
| Empirical formula | $C_{12}H_{16}CaN_2O_6S$ | $C_6H_2BaO_4S$ |
| Formula weight | 356.41 | 307.48 |
| Crystal system | Monoclinic | Monoclinic |
| Space group | *C*2/*c* | *C*2/*c* |
| *a* / nm | 1.503 47(15) | 1.929 10(19) |
| *b* / nm | 0.569 50(6) | 0.595 57(6) |
| *c* / nm | 1.792 00(18) | 0.693 01(7) |
| $\beta$ / (°) | 94.565 2(14) | 110.678(1) |
| Volume / $nm^3$ | 1.529 5(3) | 0.744 92(13) |
| *Z* | 4 | 4 |
| *F*(000) | 744 | 568 |
| Crystal size / mm | 0.32 × 0.16 × 0.05 | 0.14 × 0.08 × 0.06 |
| $D_c$ / ($g\cdot cm^{-3}$) | 1.548 | 2.742 |
| Absorption coefficient / $mm^{-1}$ | 0.576 | 5.575 |
| $\theta$ range / (°) | 3.4~30.0 | 4.5~30.1 |
| Reflection collected | 13 819 | 6 788 |
| Independent reflection ($R_{int}$) | 2 229 (0.024) | 1 102 (0.022) |
| Reflection observed [$I>2\sigma(I)$] | 2 084 | 956 |
| Data, restraint, parameter | 2 229, 0, 104 | 1 102, 5, 80 |
| Goodness-of-fit on $F^2$ | 1.080 | 1.134 |
| $R_1$, $wR_2$[a] ($I>2\sigma(I)$) | 0.027 8, 0.077 0 | 0.021 5, 0.053 8 |
| $R_1$, $wR_2$[b] (all data) | 0.029 6, 0.078 7 | 0.025 4, 0.058 8 |
| Largest diff. peak and hole / ($e\cdot nm^{-3}$) | 396 and −197 | 2 385 and 516 |

[a]$R_1=\sum||F_o|-|F_c||/\sum|F_o|$; [b]$wR_2=[\sum w(F_o^2-F_c^2)/\sum w(F_o^2)^2]^{1/2}$

**Table 2 Selected bond lengths (nm) and angles (°) for complexes 1 and 2**

| | | | | | |
|---|---|---|---|---|---|
| **1** | | | | | |
| Ca1-O1 | 0.235 77(7) | Ca1-O3 | 0.234 19(9) | O3-C4 | 0.124 23(15) |
| Ca1-O1$^{i}$ | 0.235 78(7) | Ca1-O2$^{ii}$ | 0.236 22(8) | N1-C5 | 0.144 95(17) |
| Ca1-O3$^{i}$ | 0.234 19(9) | Ca1-O2$^{iii}$ | 0.236 22(8) | S1-C1 | 0.171 60(10) |
| N1-C4 | 0.132 09(14) | N1-C6 | 0.144 63(17) | | |
| O3-Ca1-O1 | 92.79(3) | O1-Ca1-O1$^{i}$ | 180.0 | C2-O1-Ca1 | 142.75(7) |
| O3-Ca1-O1$^{i}$ | 87.21(3) | O3-Ca1-O2$^{ii}$ | 94.01(3) | C1-S1-C1$^{iv}$ | 92.27(7) |
| O1-Ca1-O2$^{iii}$ | 98.57(3) | O1$^{i}$-Ca1-O2$^{iii}$ | 81.43(3) | O3-Ca1-O2$^{iii}$ | 85.99(3) |
| **2** | | | | | |
| Ba1-O2$^{i}$ | 0.264 6(2) | Ba1-O1$^{iii}$ | 0.2721(3) | Ba1-O2$^{v}$ | 0.274 8(3) |
| Ba1-O2$^{ii}$ | 0.264 6(2) | Ba1-O2 | 0.2748(3) | C1-O2 | 0.126 9(3) |
| Ba1-O1$^{iv}$ | 0.272 1(3) | S1-C2 | 0.1720(3) | C1-O1 | 0.125 7(3) |
| O1$^{iii}$-Ba1-O1$^{iv}$ | 180.00(10) | O2$^{i}$-Ba1-O1$^{iii}$ | 90.95(11) | C1-O2-Ba1 | 101.42(18) |
| O2$^{i}$-Ba1-O1$^{iv}$ | 89.05(11) | O2$^{i}$-Ba1-O2$^{v}$ | 95.78(7) | C1-O2-Ba1$^{iv}$ | 139.1(2) |
| O2$^{ii}$-Ba1-O2$^{v}$ | 84.22(7) | O2$^{ii}$-Ba1-O1$^{iv}$ | 90.95(11) | Ba1$^{ii}$-O1-Ba1 | 101.51(9) |
| O1$^{iii}$-Ba1-O2$^{v}$ | 73.84(9) | C1-O1-Ba1 | 82.3(2) | O1$^{iv}$-Ba1-O2$^{v}$ | 106.16(9) |
| C2-S1-C2$^{vi}$ | 91.49(19) | Ba1$^{iv}$-O2-Ba1 | 115.77(9) | C1-O1-Ba1$^{ii}$ | 135.8(3) |

Symmetry codes: $^{i}$ $-x+1, -y+1, -z+1$; $^{ii}$ $-x+1, -y, -z+1$; $^{iii}$ $x, y+1, z$; $^{iv}$ $-x+1, y, -z+1/2$; $^{v}$ $x, y-1, z$ for **1**; $^{i}$ $x, -y, z-1/2$; $^{ii}$ $-x+1/2, y+1/2, -z+1/2$; $^{iii}$ $x, -y+1, z-1/2$; $^{iv}$ $-x+1/2, y-1/2, -z+1/2$; $^{v}$ $-x+1/2, -y+1/2, -z$; $^{vi}$ $-x+1, y, -z+3/2$ for **2**.

## 2 Results and discussion

### 2.1 Crystal structure of $[Ca(tdc)(DMF)_2]_n$ (1)

Single-crystal X-ray analysis reveals that the complex **1** crystallizes in a monoclinic system with space group *C*2/*c*. As shown in Fig.1a, the asymmetric unit of **1** contains one Ca(Ⅱ) ion, one $tdc^{2-}$ anion and two coordinated DMF molecules. Each Ca(Ⅱ) ion acquires a distorted octahedral geometry, which is provided by four carboxylate oxygen atoms from four different $tdc^{2-}$ moieties which are occupied in the equatorial position and other two oxygen atoms from the coordinated DMF molecules in the axial position. The bond lengths of equatorial plane are 0.235 77(7) nm (Ca1-O1) and 0.236 22(8) nm (Ca1-O2) respectively. The axial Ca1-O3 bond length is 0.234 19(9) nm. The bond angles around the Ca(Ⅱ) center are lying in the range of 81.43(3)°~180.00(3)°. In **1**, each $tdc^{2-}$ anion adopts $\mu_4$-$\eta^1$:$\eta^1$:$\eta^1$:$\eta^1$ bis-bidentate coordination mode (Scheme 1, mode Ⅰ), connecting four Ca(Ⅱ) ions to form an infinite one dimensional chain along the *c* axis, and the Ca⋯Ca distance across the bridging $tdc^{2-}$ is 0.896 00(9) nm. Further the 1D chains are linked together by carboxylate groups from two individual $tdc^{2-}$ ligands down the *b* direction generating a two-dimensional (2D) layer (Fig.1b). The neighboring Ca ions are separated by 0.569 50(6) nm. If the Ca(Ⅱ) ion is simplified as a 4-connected node and $tdc^{2-}$ ligand is considered as linear linker, thus the structure of **1** can be described as a 4-connected uninodal net with Schläfli symbol of $(4^4\cdot6^2)$ (Fig.1c).

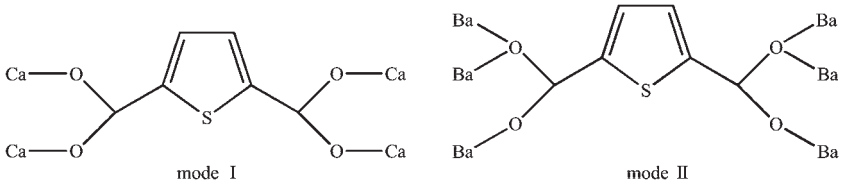


Scheme 1 Coordination modes of the $tdc^{2-}$ ligand in complexes **1** and **2**

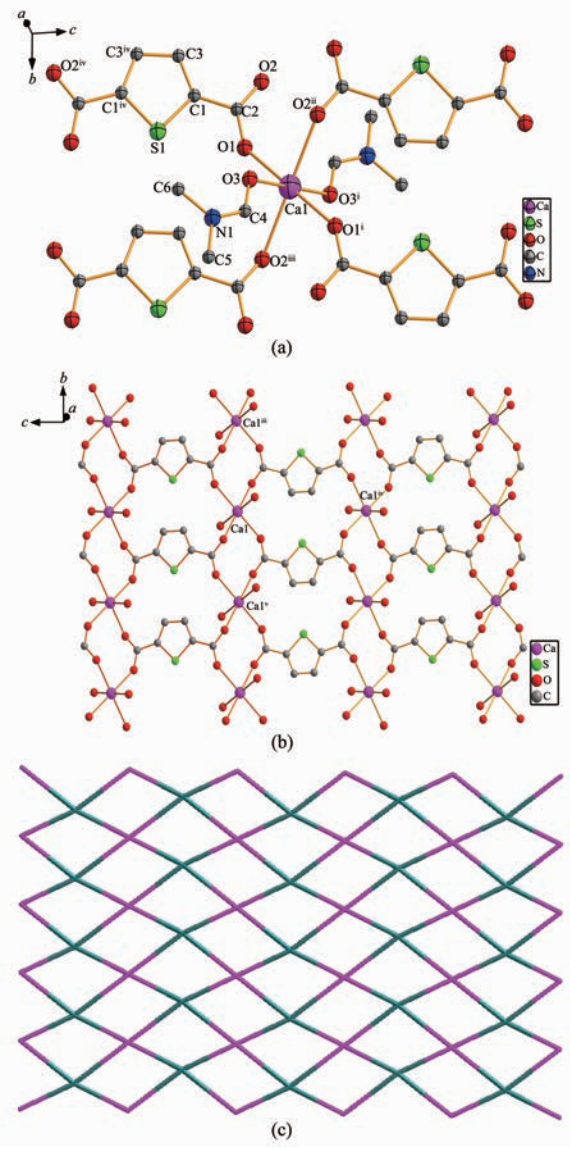


Thermal ellipsoids are shown at the 30% probability level; H atoms are omitted for clarity; Symmetry codes: [i] $-x+1, -y+1, -z+1$; [ii] $-x+1, -y, -z+1$; [iii] $x, y+1, z$; [iv] $-x+1, y, -z+1/2$; [v] $x, y-1, z$ in (a); Coordinated DMF are simplified for clarity

Fig.1　(a) Coordination environment of Ca(Ⅱ) center in complex **1**; (b) View of the 2D layer structure along the *a* axis; (c) Schematic view of the 4-connected net in **1** (teal nodes for $tdc^{2-}$ ligand and purple nodes for Ca(Ⅱ) centers

## 2.2　Crystal structure of $[Ba(tdc)]_n$ (2)

Complex **2** crystallizes in the monoclinic system, with *C*2/*c* space group. As illustrated in Fig.2a, the asymmetric unit of **2** is composed of one Ba(Ⅱ) ion and one $tdc^{2-}$ anion. Each Ba(Ⅱ) center is hexa-coordinated with the contribution of the six carboxylate oxygen atoms from six different $tdc^{2-}$ ligands which results a distorted octahedral geometry. The Ba-O bond lengths are measured in the range of 0.264 59(2)~0.274 78(2) nm, and the bond angles around the Ba(Ⅱ) center are lying in the range of 73.84(9)°~180.0(1)°. In **2**, The $tdc^{2-}$ ligand displays coordination modes $\mu_6$-$\eta^1$:$\eta^2$:$\eta^1$:$\eta^2$ to bridge six Ba(Ⅱ) ions through its four oxygen atoms (Scheme 1, mode Ⅱ), which are different from those in **1**. The identical Ba(Ⅱ) ions are bridged by the $\mu_3$-$\eta^1$:$\eta^2$-$tdc^{2-}$ ligands to form a 2D layer on the bc plane, and the neighboring Ba⋯Ba distance are 0.456 88(3) nm for Ba1-Ba1[ii] and 0.595 57(6) nm for Ba1[ii]-Ba1[iv] (Fig.2b). Furthermore, the adjacent layers are interco-

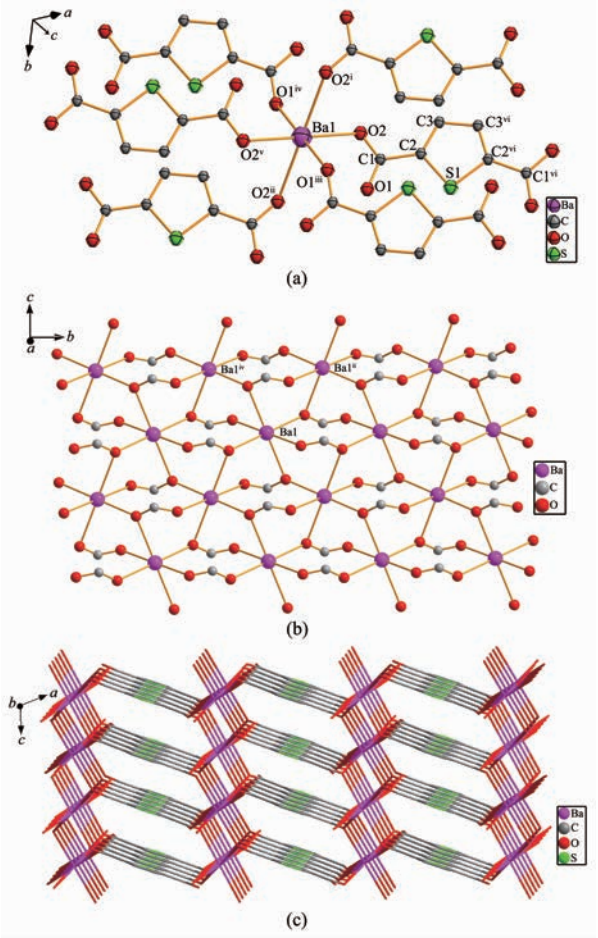


Thermal ellipsoids are shown at the 30% probability level; H atoms are omitted for clarity; Symmetry codes: [i] $x, -y, z-1/2$; [ii] $-x+1/2, y+1/2, -z+1/2$; [iii] $x, -y+1, z-1/2$; [iv] $-x+1/2, y-1/2, -z+1/2$; [v] $-x+1/2, -y+1/2, -z$; [vi] $-x+1, y, -z+3/2$

Fig.2　(a) Coordination environment of Ba(Ⅱ) center in complex **2**; (b) View of the 2D layer structure along the *a* axis; (c) 3D framework of complex **2** along the *b* axis

nnected through the $tdc^{2-}$ ligands to generate a 3D extended network consisting of elongated hexagonal channels with approximate dimensions of 1.013 52 nm×0.792 17 nm (diagonal distances).

### 2.3 Thermal stabilities and powder X-ray diffraction

To investigate the stability of the complexes **1** and **2**, thermogravimetric analysis (TGA) experiments have been performed on single crystal samples under $N_2$ atmosphere. As shown in Fig.3, the TGA curve of complex **1** exhibits an initial weight loss (19.2%) between 30 and 450 ℃, corresponding to the release of coordinated DMF solvent molecules. Then the significant weight loss occurred from 450 to 500 ℃, which could be attributable to the decomposition of the organic ligand $tdc^{2-}$. Unlike **1**, Complex **2** is stable up to 450 ℃ and undergoes an abrupt weight loss (30.2%) in the temperature range of 450~550 ℃, which corresponds to the collapse of the main framework. The final residues are detected with the weight

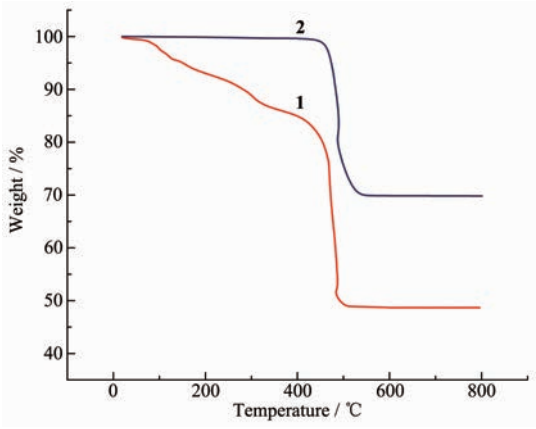


Fig.3 TGA curves for the complexes **1** and **2**

of 48.67% for **1** and 69.8% for **2**.

In order to confirm the phase purity of the bulk materials, powder X-ray diffraction (PXRD) experiments were carried out on complexes **1** and **2** at room temperature. The experimental PXRD patterns (Fig.4) are in good agreement with the corresponding simulated ones except for the relative intensity because of the preferred orientations of the crystals.

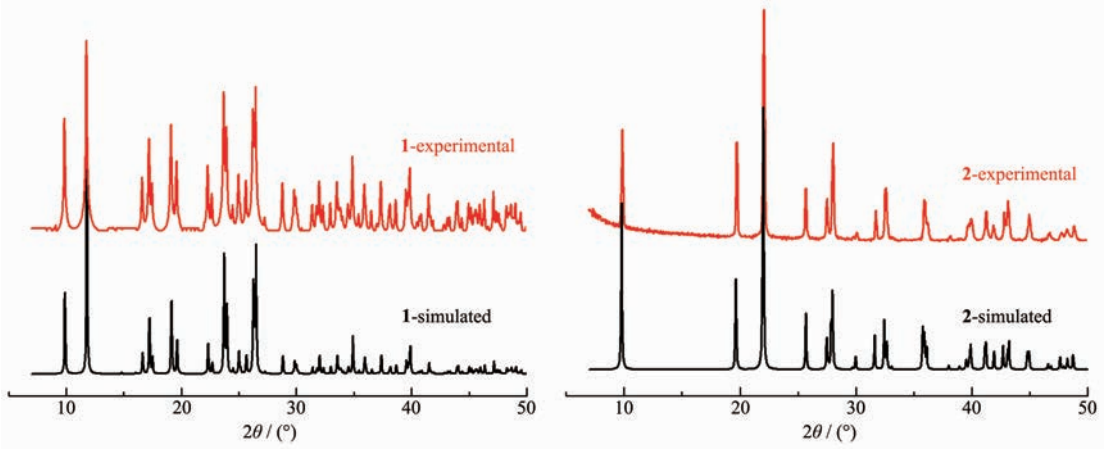


Fig.4 PXRD patterns of the complexes **1** and **2**

### 2.4 Photoluminescent properties

Photoluminescent coordination polymers have aroused great interest with their various applications in chemical sensors, photochemistry and electroluminescent display[34-35]. Therefore, the luminescent properties of complexes **1** and **2**, as well as free $H_2tdc$ ligand were investigated in solid state at room temperature. As shown in Fig.5, the free $H_2tdc$ ligand shows a wide emission band in the range of 325~375 nm with a maximum at 344 nm ($\lambda_{ex}$=302 nm), which may be attributed to the $\pi^*\rightarrow n$ or $\pi^*\rightarrow\pi$ transition[36-37]. Upon an excitation band at 302 nm, intense emissions are observed at 350 nm for **1** and 354 nm for **2**, respectively. The emissions for the two complexes are quite similar to that of the free $H_2tdc$ ligand in terms of position and band shape. The enhancement of luminescence intensity compared to the free ligand perhaps result from the coordination interactions of the ligand to the metal center, which effectively increases the rigidity of the ligand and reduces the

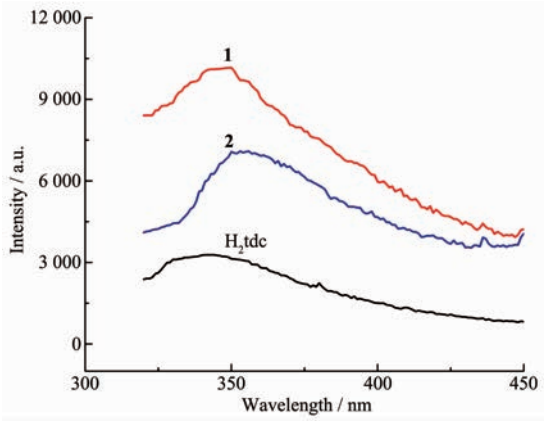


Fig.5　Solid-state emission spectra of $H_2$tdc ligand and complexes **1** and **2** at room temperature

loss of energy by radiationless decay[38-39]. Moreover, it can be seen that the calcium complex exhibits stronger emission intensity than the barium complex even the same ligand has been used, which might be resulted from the coordination mode diversities of the ligand and difference of metal ion radii.

## 3　Conclusions

In summary, two new alkaline earth metal coordination polymers based on 2,5-thiophene dicarboxylate ligand have been successfully synthesized and characterized. The crystal structural analyses indicate that complex **1** possesses a two-dimensional (2D) layer structure because the solvent DMF participate in the coordination and restricts the extension of the polymer to form 3D network. In complex **2**, the metal ions organized by $tdc^{2-}$ ligand giving rise to a fascinating 3D framework. Thermogravimetric analysis reveals that complex **2** shows better thermal stability than complex **1**. In addition, Complex **1** exhibits stronger emission energy than complex **2** which may be due to the coordination diversities of the ligand and the rigid differences of the two coordination frameworks. The results demonstrate that coordination mode, solvents, and metal centers are critical to the assemblies of MOCPs in some systems. Further experiments exploring the effect of selectivity of the auxiliary ligand, temperature, pH value and other subtle reaction condition changes on coordination polymers, are underway in our laboratory.

## References:

[1] Zhang Z J, Nguyen H T H, Miller S A, et al. *Angew. Chem. Int. Ed.*, **2015**,**54**:6152-6157

[2] Kiyonaga T, Higuchi M, Kajiwara T, et al. *Chem. Commun.*, **2015**,**51**:2728-2730

[3] Lin R B, Li T Y, Zhou H L, et al. *Chem. Sci.*, **2015**,**6**:2516-2521

[4] Maheswaran S, Chastanet G, Teat S J, et al. *Angew. Chem. Int. Ed.*, **2005**,**44**:5044-5048

[5] Manna K, Zhang T, Greene F X, et al. *J. Am. Chem. Soc.*, **2015**,**137**:2665-2673

[6] Cui Y J, Xu H, Yue Y F, et al. *J. Am. Chem. Soc.*, **2012**, **134**:3979-3982

[7] Rocha J, Carlos L D, Almeida Paz F A, et al. *Chem. Soc. Rev.*, **2011**,**40**:926-940

[8] LI Cheng-Juan(李成娟), YAN Cai-Xin(燕彩鑫), YANG Xin-Xin(杨欣欣), et al. *Chinese J. Inorg. Chem.*(无机化学学报), **2016**,**32**(5):891-898

[9] Li J R, Sculley J, Zhou H C. *Chem. Rev.*, **2012**,**112**:869-932

[10]Talin A A, Centrone A, Ford A C. *Science.*, **2014**,**343**:66-69

[11]Zheng Y Z, Evangelisti M, Funa F. *J. Am. Chem. Soc.*, **2012**,**134**:1057-1065

[12]LIU Yong-Min(刘永民), XU Ling-Ling(徐玲玲), ZHU Yu(朱禹), et al. *Chinese J. Inorg. Chem.*(无机化学学报), **2014**,**30** (12):2879-2886

[13]Zou J Y, Xu N, Shi W, et al. *RSC Adv.*, **2013**,**3**:21511-21516

[14]Jia H L, Li Y L, Xiong Z F, et al. *Dalton Trans.*, **2014**,**43**: 3704-3715

[15]Yang M, Jiang F L, Chen Q H, et al. *CrystEngComm*, **2011**, **13**:3971-3974

[16]MA Zhi-Feng(马志峰), ZHANG Ying-Hui(章应辉), HU Tong-Liang(胡同亮), et al. *Chinese J. Inorg. Chem.*(无机化学学报), **2014**,**30**(1):204-212

[17]Wang X S, Ma S Q, Rauch K, et al. *Chem. Mater.*, **2008**,**20**: 3145-3152

[18]OU Yong-Cong(区泳聪), ZHONG Jun-Xing(钟均星), SONG Ying-Yi(宋萦怡). *Chinese J. Inorg. Chem.*(无机化学学报), **2016**,**32**(4):738-744

[19]He H J, Zhang L N, Deng M L, et al. *CrystEngComm*, **2015**, **17**:2294-2300

[20]Venkateswarulu M, Pramanik A, Koner R R. *Dalton Trans.*, **2015**,**44**:6348-6352

[21]XU Han(徐 涵), ZHENG He-Gen(郑和根). *Chinese J. Inorg. Chem.*(无机化学学报), **2016**,**32**(1):184-190

[22]Li J R, Zhou H C. *Angew. Chem. Int. Ed.*, **2009**,**48**:8465-8468

[23]Zhou L, Wang C G, Zheng X F, et al. *Dalton Trans.*, **2013**, **42**:16375-16386

[24]Wang H, Yi F Y, Dang S, et al. *Cryst. Growth Des.*, **2014**, **14**:147-156

[25]Parshamoni S, Sanda S, Jena H S, et al. *Dalton Trans.*, **2014**, **43**:7191-7199

[26]Thangavelu S G, Butcher R J, Cahill C L. *Cryst. Growth Des.*, **2015**,**15**:3481-3492

[27]Kettner F, Worch C, Moellmer J. *Inorg. Chem.*, **2013**,**52**: 8738-8742

[28]Sun Y G, Jiang B, Cui T F, et al. *Dalton Trans.*, **2011**,**40**: 11581-11590

[29]Chen X Y, Plonka A M, Banerjee D, et al. *Cryst. Growth Des.*, **2013**,**13**:326-332

[30]Fromm K M. *Coord. Chem. Rev.*, **2008**,**252**:856-885

[31]Yang L M, Ravindran P, Vajeeston P, et al. *RSC Adv.*, **2012**, **2**:1618-1631

[32]Schmidbaur H, Mikulik P, Müller G. *Chem. Ber.*, **1990**,**123**: 1599-1602

[33]Sheldrick G M. *SADABS*, *Program for Empirical Absorption Correction of Area Detector Data*, University of Göttingen, Germany, **2014**.

[34]Sheldrick G M. *SHELXL*-2014, *Program for Crystal Structure Refinement*, University of Göttingen, Germany, **2014**.

[35]Cui Y J, Yue Y F, Qian G D, et al. *Chem. Rev.*, **2012**,**112**: 1126-1162

[36]Hu Z C, Deibert B J, Li J. *Chem. Soc. Rev.*, **2014**,**43**:5815-5840

[37]Parshamoni S, Sanda S, Jena H S, et al. *Cryst. Growth Des.*, **2014**,**14**:2022-2033

[38]Qiao J Z, Zhan M S, Hu T P. *RSC Adv.*, **2014**,**4**:62285-62294

[39]Tomar K, Rajak R, Sanda S, et al. *Cryst. Growth Des.*, **2015**, **15**:2732-2741

[40]Zhang Y, Guo B B, Li L, et al. *Cryst. Growth Des.*, **2013**,**13**: 367-376